

A new Size REsolved Aerosol Model

E. Debry et al.

Technical Note: A new Size REsolved Aerosol Model (SIREAM)

E. Debry, K. Fahey, K. Sartelet, B. Sportisse, and M. Tombette

CEREA, Joint Research Laboratory, École Nationale des Ponts et Chaussées/EDF R&D,
France

Received: 9 November 2006 – Accepted: 14 November 2006 – Published: 22 November 2006

Correspondence to: B. Sportisse (bruno.sportisse@cerea.enpc.fr)

Title Page

Abstract

Introduction

Conclusions

References

Tables

Figures

◀

▶

◀

▶

Back

Close

Full Screen / Esc

Printer-friendly Version

Interactive Discussion

EGU

Abstract

We briefly present in this short paper a new Size REsolved Aerosol Model (SIREAM) which simulates the evolution of atmospheric aerosol by solving the General Dynamic Equation (GDE). SIREAM segregates the aerosol size distribution into sections and solves the GDE by splitting coagulation and condensation/evaporation. A moving sectional approach is used to describe the size distribution change due to condensation/evaporation and a hybrid method has been developed to lower the computational burden. SIREAM uses the same physical parameterizations as those used in the Modal Aerosol Model, MAM (Sartelet et al., 2005). It is hosted in the modeling system POLYPHEMUS (Mallet et al., 2006¹) but can be linked to any other three-dimensional Chemistry-Transport Model.

1 Introduction

Atmospheric particulate matter (PM) has been negatively linked to a number of undesirable phenomena ranging from visibility reduction to adverse health effects. It also has a strong influence on the earth's energy balance (Seinfeld and Pandis, 1998). As a result, many governing bodies, especially in North America and Europe, have imposed increasingly stringent standards for PM.

Atmospheric aerosol is a complex mixture of inorganic and organic components, with composition varying over the size range of a few nanometers to several micrometers. These particles can be emitted directly from various anthropogenic and biogenic sources or can be formed in the atmosphere by organic or inorganic precursor gases.

Given the complexity of PM, its negative effects, and the desire to control atmospheric PM concentrations, models that accurately describe the important processes

¹Mallet, V., Quélo, D., Sportisse, B., Debry, E., Korsakissok, I., Roustan, I., Sartelet, K., Wu, L., Tombette, M., and Foudhil, H.: A new air quality modeling system: POLYPHEMUS, Atmos. Chem. Phys. Discuss., in preparation, 2006.

A new Size REsolved Aerosol Model

E. Debry et al.

Title Page

Abstract

Introduction

Conclusions

References

Tables

Figures

◀

▶

◀

▶

Back

Close

Full Screen / Esc

Printer-friendly Version

Interactive Discussion

that affect the aerosol size/composition distribution are therefore crucial. Three-dimensional Chemistry-Transport Models (CTMs) provide the necessary tools to develop not only a better understanding of the formation and the distribution of PM but also sound strategies to control it. Historically, CTMs focused on ozone formation or acid deposition and did not include a detailed treatment of aerosols. A number of these models have been updated to include aerosols, but there are still many limitations (Seigneur, 2001).

In rigorous models that seek to describe the time and spatial evolution of atmospheric PM, it is necessary to include those processes described in the General Dynamic Equation for aerosols (condensation/evaporation, coagulation, nucleation, inorganic and organic thermodynamics). These and additional processes like heterogeneous reactions at the aerosol surface, mass transfer between aerosol and cloud droplets, and aqueous-phase chemistry inside cloud droplets represent some of the most important mechanisms for altering the aerosol size/composition distribution.

Among the aerosol models, one usually distinguishes between “modal” models (Whitby and McMurry, 1997) and “size resolved” or “sectional” models (Gelbard et al., 1980). We refer for instance to the modal model of Binkowski and Roselle (2003) and the sectional model of Zhang et al. (2004) for a description of state-of-the-science aerosol models, hosted by the Chemistry-Transport Model, CMAQ (Byun and Schere, 2004).

Here we present the development of a new Size REsolved Aerosol Model (SIREAM). SIREAM is strongly coupled to a “companion” modal model, MAM (Modal Aerosol Model, Sartelet et al., 2005). Both models utilize the same physical parameterizations through the library for atmospheric physics and chemistry ATMODATA (Mallet and Sportisse, 2005). Both have a modular approach and rely on different model configurations. They are hosted in the modeling system POLYPHEMUS (Mallet et al., 2006¹) and used in many applications. A detailed description of SIREAM and MAM can be found in Sportisse et al. (2006) (available at <http://www.enpc.fr/cerea/polypphemus>). A key feature of SIREAM is its modular design, as opposed to an all-in-one model.

A new Size REsolved Aerosol Model

E. Debry et al.

[Title Page](#)[Abstract](#)[Introduction](#)[Conclusions](#)[References](#)[Tables](#)[Figures](#)[I◀](#)[▶I](#)[◀](#)[▶](#)[Back](#)[Close](#)[Full Screen / Esc](#)[Printer-friendly Version](#)[Interactive Discussion](#)

SIREAM can be used in many configurations and is intended for ensemble modeling (similar to [Mallet and Sportisse, 2006](#)).

This paper is structured as follows. The model formulation and main parameterizations included in SIREAM are described in Sect. 2. The numerical algorithms used for solving the GDE are given in Sect. 3. A specific focus is devoted to condensation/evaporation, which is by far the most challenging issue.

2 Model formulation

In this section we focus on aerosol dynamics, i.e. on the nucleation, condensation/evaporation, and coagulation processes. In addition, we briefly describe some processes that are strongly related to aerosols (heterogeneous reactions at the aerosol surface, mass transfer between the aerosols and the cloud droplets and aqueous-phase chemistry in cloud droplets). We also include the parameterizations for Semi-Volatile Organic Compounds (SVOCs).

In order to deal with different parameterizations and to avoid the development of an “all-in-one” model, the parameterizations have been implemented as functions of the library ATMODATA ([Mallet and Sportisse, 2005](#)), a package for atmospheric physics. As such, they can be used by other models.

2.1 Composition

The particles are assumed to be “internally mixed”, i.e., that there is a unique chemical composition for a given size. Each aerosol may be composed of the following components:

- liquid water;
- inert species: mineral dust, elemental carbon and, in some applications, heavy trace metals (lead, cadmium) or radionuclides bound to aerosols;

Title Page

Abstract

Introduction

Conclusions

References

Tables

Figures

◀

▶

◀

▶

Back

Close

Full Screen / Esc

Printer-friendly Version

Interactive Discussion

- inorganic species: Na^+ , SO_4^{2-} , NH_4^+ , NO_3^- and Cl^- ;
- organic species: one species for “Primary Organic Aerosol” (POA), 8 species for Secondary Organic Aerosol (see below for more details).

A typical version of the model (trace metals or radionuclides are not included) tracks the evolution of 17 chemical species for a given size bin (1+2+5+1+8). These species (“external species”) should be distinguished from the species that are actually inside one aerosol in different forms (ionic, dissolved, solid). Let n_e be the number of external species.

The internal composition for inorganic species is determined by thermodynamic equilibrium, solved by ISORROPIA v.1.7 (Nenes et al., 1998). Water is assumed to quickly reach equilibrium between the gas and aerosol phases. Its concentration is given by the thermodynamic model (through the Zdanovskii-Stokes-Robinson relation).

Hereafter, the particle mass m refers to the dry mass. In order to reduce the wide range of magnitude over the particle size distribution and to better represent small particles, the particle distribution is described with respect to the logarithmic mass $x = \ln m$ (Wexler et al., 1994; Meng et al., 1998; Gaydos et al., 2003).

The particles are described by a number distribution, $n(x, t)$ (in m^{-3}), and by the mass distributions for species X_i , $\{q_i(x, t)\}_{i=1, n_e}$ (in $\mu\text{g m}^{-3}$). The mass distributions satisfy $\sum_{i=1}^{i=n_e} q_i = m n$. We also define the mass $m_i(x, t) = \frac{q_i(x, t)}{n(x, t)}$ of species X_i in the particle of logarithmic mass x . It satisfies $\sum_{i=1}^{i=n_e} m_i(x, t) = e^x$.

2.2 Processes and parameterizations for the GDE

2.2.1 Nucleation

The formation of the smallest particles is given by the aggregation of gaseous molecules leading to thermodynamically stable “clusters”. The mechanism is poorly known and most models assume homogeneous binary nucleation of sulfate and water

A new Size REsolved Aerosol Model

E. Debry et al.

Title Page

Abstract

Introduction

Conclusions

References

Tables

Figures

◀

▶

◀

▶

Back

Close

Full Screen / Esc

Printer-friendly Version

Interactive Discussion

to be the major mechanism in the formation of new particles. Binary schemes tend to underpredict nucleation rates in comparison with observed values. [Korhonen et al. \(2003\)](#) has indicated that for the conditions typical in the lower troposphere ternary nucleation of sulfate, ammonium and water may be the only relevant mechanism.

5 SIREAM offers two options for nucleation: the H₂O-H₂SO₄ binary nucleation scheme of [Vehkamäki et al. \(2002\)](#) and the H₂O-H₂SO₄-NH₃ ternary nucleation scheme of [Napari et al. \(2002\)](#).

The output is a nucleation rate, J_0 , a nucleation diameter, and chemical composition for the nucleated particles. The new particles are added to the smallest bin.

10 2.2.2 Coagulation

Atmospheric particles may collide with one another due to their Brownian motion or due to other forces (e.g., hydrodynamic, electrical or gravitational). SIREAM includes a description of Brownian coagulation, the dominant mechanism in the atmosphere. There may be a limited effect on the particle mass distribution and this process is usually neglected ([Zhang et al., 2004](#)). However coagulation may have substantial impact on the number size distribution for ultrafine particles.

15 The coagulation kernel $K(x, y)$ (in unit of volume per unit of time) describes the rate of coagulation between two particles of dry logarithmic masses x and y . K has different expressions depending on the relevant regime ([Seinfeld and Pandis, 1998](#)).

20 2.2.3 Condensation/evaporation

Some gas-phase species with a low saturation vapor pressure may condense on existing particles while some species in the particle phase may evaporate. The mass transfer is governed by the gradient between the gas-phase concentration and the concentration at the surface of the particle. The mass flux for volatile species X_i between

Title Page

Abstract

Introduction

Conclusions

References

Tables

Figures

◀

▶

◀

▶

Back

Close

Full Screen / Esc

Printer-friendly Version

Interactive Discussion

the gas phase and one particle of logarithmic mass x is computed by:

$$\frac{dm_i}{dt} = I_i = 2\pi D_i^g d_p f_{FS}(K_{n_i}, \alpha_i) \left(c_i^g - c_i^s(x, t) \right) \quad (1)$$

d_p is the particle wet diameter. (see Sect. 2.2.6 for the relation to mass). D_i^g and c_i^g are the molecular diffusivity in the air and the gas-phase concentration of species X_i , respectively. The concentration c_i^s at the particle surface is assumed to be at local thermodynamic equilibrium with the particle composition:

$$c_i^s(x, t) = \eta(d_p) c_i^{eq}(q_1(x, t), \dots, q_{n_e}(x, t), \text{RH}, T) \quad (2)$$

T is the temperature and RH is the relative humidity. $\eta(d_p) = \exp\left(\frac{4\sigma v_p}{RT d_p}\right)$ is a correction for the Kelvin effect, with σ the surface tension, R the gas constant and v_p the particle molar volume. In practice, c_i^{eq} is computed by the reverse mode of a thermodynamics package like ISORROPIA in the case of kinetic mass transfer.

The Fuchs-Sutugin function, f_{FS} , describes the non-continuous effects (Dahneke, 1983). It depends on the Knudsen number of species X_i , $K_{n_i} = \frac{2\lambda_i}{d_p}$ (with λ_i the air mean free path), and on the accommodation coefficient α_i (default value is 0.5):

$$f_{FS}(K_{n_i}, \alpha_i) = \frac{1 + K_{n_i}}{1 + 2K_{n_i}(1 + K_{n_i})/\alpha_i} \quad (3)$$

When particles are in a liquid state, the condensation of an acidic component may free hydrogen ions and the condensation of a basic component may consume hydrogen ions. Thus the condensation/evaporation (c/e hereafter) process may have an effect on the particle pH. The hydrogen ion flux induced by mass transfer is:

$$J_{H^+} = 2J_{H_2SO_4} + J_{HCl} + J_{HNO_3} - J_{NH_3} \quad (4)$$

with J_i the molar flux in species X_i . The pH evolution due to c/e can be very stiff and cause instabilities, due to the very small quantity n_{H^+} of hydrogen ions inside the

particle. The hydrogen ion flux is then limited to a given fraction A of the hydrogen ion concentration (following [Pilinis et al., 2000](#)): $|J_{H^+}| \leq A n_{H^+}$, where A is usually chosen arbitrarily between 0.01 and 0.1. A is a numerical parameter that has no physical meaning and does not influence the final state of mass transfer. It just modifies the numerical path to reach this state. We refer to [Pilinis et al. \(2000\)](#) for a deeper understanding.

2.2.4 Inorganic thermodynamics

There are a range of packages available to solve thermodynamics for inorganic species ([Zhang et al., 2000](#)). ISORROPIA was shown to be a computationally efficient model that is also numerically accurate and stable and provides both a closed mode (for global equilibrium, a.k.a. forward mode) and open mode (for local equilibrium and kinetic mass transfer, a.k.a. reverse mode). Particles can be solid, liquid, both or in a metastable state, where particles are always in aqueous solution.

Moreover, the inclusion of sea salt (NaCl) in the computation of thermodynamics is also an option in SIREAM.

When the particles are solid, fluxes of inorganic species are governed by gas/solid reactions at the particle surface. In this case, thermodynamic models are not able to compute gas equilibrium concentrations. For solid particle, SIREAM calculations are based on the solutions proposed in [Pilinis et al. \(2000\)](#).

2.2.5 Secondary Organic Aerosols

The oxidation of VOCs leads to species (SVOCs) that have increasingly complicated chemical functions, high polarizations, and lower saturation vapor pressure.

There are many uncertainties surrounding the formation of secondary organic aerosol. Due to the lack of knowledge and the sheer number and complexity of organic species, most chemical reaction schemes for organics are very crude representations of the “true” mechanism. These typically include the lumping of “representative”

A new Size REsolved Aerosol Model

E. Debry et al.

Title Page

Abstract

Introduction

Conclusions

References

Tables

Figures

◀

▶

◀

▶

Back

Close

Full Screen / Esc

Printer-friendly Version

Interactive Discussion

organic species and highly simplified reaction mechanisms.

The default gas-phase chemical mechanism for SIREAM is RACM (Stockwell et al., 1997). Notice that the gas-phase mechanism and the related SVOCs are parameterized and can be easily modified.

5 The low volatility SOA precursors and the partitioning between the gas and particle phases are based on the empirical SORGAM model (Schell et al., 2001; Schell, 2000). Eight SOA classes are taken into account (4 anthropogenic and 4 biogenic). Anthropogenic species include two from aromatic precursors (ARO1 and ARO2), one from higher alkanes (OLE1) and one from higher alkenes (ALK1). The biogenic species
10 represent two classes from α -pinene (API1 and API2) and two from limonene (LIM1 and LIM2) degradation. Some oxidation reactions of the form $\text{VOC} + \text{Ox} \rightarrow \text{P}$ where Ox is OH, O₃, or NO₃ have been modified to $\text{VOC} + \text{Ox} \rightarrow \text{P} + \alpha_1 \text{P}_1 + \alpha_2 \text{P}_2$ with P₁ and P₂ representing SVOCs among the eight classes. Updated values of these parameters have also been defined in other versions of the mechanism (not reported here).

15 The partitioning between the gas phase and the particle phase is performed in the following way. Let n_{OM} be the number of organic species in the particle mixture (this includes primary and secondary species) which are assumed to constitute an “ideal mixture”:

$$(q_i)_g = \gamma_i (x_i)_a q_i^{\text{sat}} \quad (5)$$

20 For species X_i , q_i^{sat} is the saturation mass concentration in a pure mixture, $(x_i)_a$ is the molar fraction in the organic mixture and γ_i is the activity coefficient in the organic mixture (a default value of 1 is assumed). $(x_i)_a$ is computed through:

$$(x_i)_a = \frac{\frac{(q_i)_a}{M_i}}{\frac{q_{OM}}{M_{OM}}} = \frac{\frac{(q_i)_a}{M_i}}{\sum_{j=1}^{j=n_{OM}} \frac{(q_j)_a}{M_j} + \frac{(q_{\text{POA}})_a}{M_{\text{POA}}}} \quad (6)$$

A new Size REsolved Aerosol Model

E. Debry et al.

Title Page

Abstract

Introduction

Conclusions

References

Tables

Figures

◀

▶

◀

▶

Back

Close

Full Screen / Esc

Printer-friendly Version

Interactive Discussion

q_{OM} is the total concentration of organic matter (primary and secondary) in the particle phase. The molar mass M_i of component i is expressed in $\mu\text{g/mol}$ (in the same unit as the mass concentrations q_i); M_{OM} is the average molar mass for organic matter in $\mu\text{g/mol}$. POA stands for the primary organic matter, assumed not to evaporate.

- 5 q_i^{sat} is computed from the saturation vapor pressure with $q_i^{\text{sat}} = \frac{M_i}{RT} p_i^{\text{sat}}$. A similar way to proceed is to define the partitioning coefficient $K_i = \frac{(q_i)_a}{q_{OM}(q_i)_g}$ (in $\text{m}^3/\mu\text{g}$). K_i can be computed from the thermodynamic conditions and the saturation vapor pressure through:

$$K_i = \frac{RT}{p_i^{\text{sat}} \gamma_i(M_{OM})} \quad (7)$$

- 10 The saturation vapor pressure $p_i^{\text{sat}}(T)$ is given by the Clausius-Clapeyron law:

$$p_i^{\text{sat}}(T) = p_i^{\text{sat}}(298 \text{ K}) \exp \left(-\frac{\Delta H_{\text{vap}}}{R} \left(\frac{1}{T} - \frac{1}{298} \right) \right) \quad (8)$$

with ΔH_{vap} the vaporization enthalpy (in the default version, a constant value 156 kJ/mol).

- 15 The mass concentration of a gas at local equilibrium with the particle mixture is given by Eq. (5). The global equilibrium between a gas and the particle mixture is given by Eq. (5) and mass conservation for species X_i :

$$(q_i)_a + (q_i)_g = (q_i)_{\text{tot}} \quad (9)$$

- 20 with $(q_i)_{\text{tot}}$ representing the total mass concentration (for both phases) to be partitioned. This with Eq. (6) leads to a system of n_{OM} algebraic equations of second degree:

$$-a_i((q_i)_a)^2 + b_i(q_i)_a + c_i = 0 \quad (10)$$

where the coefficients depend on concentrations $\{(q_j)_a\}_{j \neq i}$ through

$$a_i = \frac{1}{M_i}, \quad b_i = \frac{q_i^{\text{sat}}}{M_i} - \Sigma_i, \quad c_i = q_i^{\text{sat}} \Sigma_i \quad \text{and} \quad \Sigma_i = \sum_{j=1, j \neq i}^{j=n_{OM}} \frac{(q_j)_a}{M_j} + \frac{(q_{\text{POA}})_a}{M_{\text{POA}}}.$$

The resulting system is solved by an iterative approach with a fixed point algorithm. Each second degree equation is solved in an exact way: the only positive root is computed for each equation of type (10).

2.2.6 Wet diameter

Parameterizations of coagulation, condensation/evaporation, dry deposition and wet scavenging depend on the particle “wet” diameter d_p . Two methods have been implemented in SIREAM to compute it, one based on thermodynamics, another on the Gerber’s Formula.

The thermodynamic method consists in using the particle internal composition $\{m_i\}$ provided by the thermodynamic model ISORROPIA. Many of aerosol models use a constant specific particle mass ρ_p (Wexler et al., 1994; Pilinis and Seinfeld, 1988) supposed to satisfy $\rho_p \frac{\pi d_p^3}{6} = \sum_{i=1}^{n_e} m_i$. In SIREAM, following Jacobson (2002), the particle

volume is split into a solid part and a liquid part: $\frac{\pi d_p^3}{6} = V_{\text{liq}} + V_{\text{sol}}$. As each solid represents one single phase, the total solid particle volume is the sum of each solid volume:

$V_{\text{sol}} = \sum_{i_s} \frac{m_{i_s}}{\rho_{i_s}^*}$, with $\rho_{i_s}^*$ the specific mass of pure component X_{i_s} . The liquid particle

phase is a concentrated mixing of inorganic species, whose volume is a non linear function of its inorganic internal composition: $V_{\text{liq}} = \sum_{i_l} V_{i_l} n_{i_l}$ where V_{i_l} is the partial molar volume of ionic or dissolved species X_{i_l} and n_{i_l} is the molar quantity in X_{i_l} . Due to some molecular processes within the mixture (e.g. volume exclusion), the partial molar volume is a function of the internal composition. However, we assume that $V_{i_l} \simeq \frac{M_{i_l}}{\rho_{i_l}^*}$

where M_{i_l} and $\rho_{i_l}^*$ are the molar mass of X_{i_l} and the specific mass of a pure liquid solution of X_{i_l} , respectively. This method is well suited for condensation/evaporation for

Title Page

Abstract

Introduction

Conclusions

References

Tables

Figures

◀

▶

◀

▶

Back

Close

Full Screen / Esc

Printer-friendly Version

Interactive Discussion

which thermodynamic computation cannot be avoided.

For other processes (coagulation, dry deposition and scavenging) the particle “wet” diameter is computed through a faster method, the Gerber’s Formula (Gerber, 1985). This one is a parameterization of the “wet” radius as a function of the dry one:

$$r_w = \left[\frac{C_1(r_d)^{C_2}}{C_3(r_d)^{C_4} - \log RH} + (r_d)^3 \right]^{\frac{1}{3}} \quad (11)$$

where r_w and r_d are respectively the wet and dry particle radius in centimeters, RH is the atmospheric relative humidity within [0, 1]. Coefficients $(C_i)_{i=1,4}$ depend on the particle type (urban, rural or marine). The C_3 coefficient is temperature dependent (T) through the Kelvin effect:

$$C_3(T) = C_3[1 + C_5(298 - T)] \quad (12)$$

We have actually modified the coefficients given by Gerber through a minimization method so that the Gerber’s Formula give results as close as possible to the “wet” diameters given by the thermodynamic method (Sportisse et al., 2006):

$$\begin{aligned} C_1 &= 0.4989, \quad C_2 = 3.0262, \quad C_3 = 0.5372 \cdot 10^{-12} \\ C_4 &= -1.3711, \quad C_5 = 0.3942 \cdot 10^{-02} \end{aligned} \quad (13)$$

The choice of which method to use (thermodynamics or Gerber’s Formula) is up to the user.

2.2.7 Logarithmic formulation for the GDE

On the basis of the parameterizations described above, the evolution of the number and mass distributions is governed by the GDE:

$$\frac{\partial n}{\partial t}(x, t) = \int_{x_0}^{\tilde{x}} K(y, z) n(y, t) n(z, t) dy$$

$$-n(x, t) \int_{x_0}^{\infty} K(x, y) n(y, t) dy - \frac{\partial(H_0 n)}{\partial x} \quad (14)$$

$$\begin{aligned} \frac{\partial q_i}{\partial t}(x, t) = & \int_{x_0}^{\tilde{x}} K(y, z) [q_i(y, t) n(z, t) + n(y, t) q_i(z, t)] dy \\ & - q_i(x, t) \int_{x_0}^{\infty} K(x, y) n(y, t) dy \\ & - \frac{\partial(H_0 q_i)}{\partial x} + (I_i n)(x, t) \end{aligned} \quad (15)$$

$H_0 = \frac{I_0}{m}$ (in s^{-1}) is the logarithmic growth rate. The nucleation threshold is $x_0 = \ln m_0$. Moreover, $\tilde{x} = \ln(e^x - e^{x_0})$ and $z = \ln(e^x - e^y)$ in the above formula.

At the nucleation threshold, the nucleation rate determines the boundary condition:

$$(H_0 n)(x_0, t) = J_0(t), \quad (H_0 q_i)(x_0, t) = m_i(x_0, t) J_0(t) \quad (16)$$

10 The evolution of the gaseous concentration for the semi-volatile species X_i is given by:

$$\frac{dc_i^g}{dt}(t) = -m_i(x_0, t) J_0(t) - \int_{x_0}^{\infty} (I_i n)(x, t) dx \quad (17)$$

or by mass conservation: $c_i^g(t) + \int_{x_0}^{\infty} q_i(x, t) dx = K_i$.

2.3 Other processes related to aerosols

15 The following processes are not directly related to the GDE. As such, the kernel of SIREAM (the parameterizations and the algorithms for the GDE) is independent. As for SOA, other parameterizations can be used. For the sake of completeness, we have chosen to include a brief description of the default current parameterizations.

2.3.1 Mass transfer and aqueous-phase chemistry for cloud droplets

For cells with a liquid water content exceeding a critical value (the default value is 0.05 g/m^3), the grid cell is assumed to contain a cloud and the aqueous-phase module is called instead of the GDE model. A part of the particle distribution is activated for particles that exceed a critical diameter (the default value is $d_{\text{activ}} = 0.7 \mu\text{m}$). The micro-physical processes that govern the evolution of cloud droplets are parameterized and not explicitly described. Cloud droplets form on activated particles and evaporate instantaneously (during one numerical timestep) in order to take into account the impact of aqueous-phase chemistry for the activated part of the particle distribution (Fahey, 2003; Fahey and Pandis, 2001).

In order to lower the computational burden, the activated distribution is a monomodal distribution of median diameter $0.4 \mu\text{m}$ and of variance $1.8 \mu\text{m}$. The activated particle distribution is mapped onto this distribution. The tests in Fahey (2003) illustrate the low impact of the choice made for this distribution. The chemical composition of the cloud droplet is then given by the activated particle fraction.

Aqueous-phase chemistry and mass transfer between the gaseous phase and the cloud droplets are then solved. Part of the mass transfer is solved dynamically, part is assumed to have reached Henry's equilibrium. The aqueous-phase model is based on the chemical mechanism developed at Carnegie Mellon University (Strader et al., 1998). It contains 18 gas-phase species and 28 aqueous-phase species. Aqueous-phase chemistry is modeled by a chemical mechanism of 99 chemical reactions and 17 equilibria (for ionic dissociation). The radical chemistry is not taken into account. The computation of H^+ is made with the electroneutrality relation written as $f_{\text{electroneutrality}}(\text{H}^+) = 0$. This nonlinear algebraic equation is solved with the bisection method. If no convergence occurs, we take a default value $\text{pH} = 4.16$.

After one timestep, the cloud droplet distribution is then mapped to the initial particle distribution.

We use a splitting method, the gas-phase chemistry being solved elsewhere (in the

Title Page

Abstract

Introduction

Conclusions

References

Tables

Figures

◀

▶

◀

▶

Back

Close

Full Screen / Esc

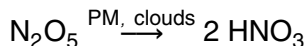
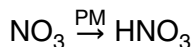
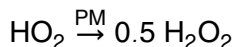
Printer-friendly Version

Interactive Discussion

gas-phase module of the Chemistry-Transport Model). Aqueous-phase chemistry and mass transfer are solved with DVODE (Brown et al., 1989).

2.3.2 Heterogeneous reactions

The heterogeneous reactions at the surface of condensed matter (particles and cloud or fog droplets) may significantly impact gas-phase photochemistry and particles. Following Jacob (2000), these processes are described by the first-order reactions:



The heterogeneous reactions for HO₂, NO₂ and NO₃ at the surface of cloud droplets are assumed to be taken into account in the aqueous-phase model and are considered separately.

The first-order kinetic rate is computed for gas-phase species X_i with $k_i = \left(\frac{a}{D_i^g} + \frac{4}{\bar{c}_i^g \gamma} \right)^{-1} S_a$ where a is the particle radius, \bar{c}_i^g the thermal velocity in the air, γ the reaction probability and S_a the available surface for condensed matter per air volume.

γ strongly depends on the chemical composition and on the particle size. We have decided to keep the variation ranges (from Jacob, 2000) for these parameters in order to evaluate the resulting uncertainties: $\gamma_{\text{HO}_2} \in [0.1-1]$, $\gamma_{\text{NO}_2} \in [10^{-6}-10^{-3}]$, $\gamma_{\text{NO}_3} \in [2 \cdot 10^{-4}-10^{-2}]$ and $\gamma_{\text{N}_2\text{O}_5} \in [0.01-1]$. The default values are the lowest values. For numerical stability requirements, these reactions are coupled to the gas-phase mechanism.

Title Page

Abstract

Introduction

Conclusions

References

Tables

Figures

◀

▶

◀

▶

Back

Close

Full Screen / Esc

Printer-friendly Version

Interactive Discussion

3 Numerical simulation

3.1 Numerical strategy

On the basis of a comprehensive benchmark of algorithms (Debry, 2004), the numerical strategy relies on methods that ensure stability with a low CPU cost. First, we use a splitting approach for coagulation and condensation/evaporation. Second, the discretization is performed with sectional methods which remain stable even with a few discretization points, contrary to spectral methods (Sandu and Borden, 2003; Debry and Sportisse, 2006b). Third, condensation/evaporation is solved with a Lagrangian method (moving sectional method) in order to avoid the numerical diffusion associated with Eulerian schemes in the case of a small number of discretization points (typically the case in 3-D models).

The splitting sequence goes from the slowest process to the fastest one (first coagulation and then condensation/evaporation-nucleation). The nucleation process is not a numerical issue and is solved simultaneously with condensation/evaporation. In the following, we present the numerical algorithm used for each process.

The particle mass distribution is discretized into n_b bins $[x^j, x^{j+1}]$. We define the integrated quantities over the bin j for the number distribution and the mass distributions for species X_i :

$$N^j(t) = \int_{x^j}^{x^{j+1}} n(x, t) dx, \quad Q_i^j = \int_{x^j}^{x^{j+1}} q_i(x, t) dx \quad (18)$$

$\tilde{m}_i^j = \frac{Q_i^j}{N^j}$ is the average mass per particle inside bin j for species X_i .

We use a Method of Lines by first performing size discretization and then time integration. After discretization, the resulting system of Ordinary Differential Equations (ODEs) has the generic form:

$$\frac{dc}{dt} = f(c, t) \quad (19)$$

A new Size REsolved Aerosol Model

E. Debry et al.

Title Page

Abstract

Introduction

Conclusions

References

Tables

Figures

◀

▶

◀

▶

Back

Close

Full Screen / Esc

Printer-friendly Version

Interactive Discussion

where the state vector c is specific for each process. c_n is the numerical approximation of $c(t_n)$ at time t_n , with a timestep $\Delta t_n = t_{n+1} - t_n$. A second-order solver is specified for each case with a first-order approximation \tilde{c}_{n+1} . The variable timestep Δt_n is adjusted by:

$$\Delta t_{n+1} = \Delta t_n \sqrt{\frac{\varepsilon_r \|c_{n+1}\|_2}{\|\tilde{c}_{n+1} - c_{n+1}\|_2}} \quad (20)$$

where ε_r is a user parameter, usually between 0.01 and 0.5. The higher ε_r is, the faster Δt_n increases. $\|\cdot\|_2$ is the Euclidean norm.

3.2 Size discretization

3.2.1 Coagulation

Coagulation is solved by the so-called “size binning” method. Equations (14) and (15) are integrated over each bin, which gives:

$$\begin{aligned} \frac{dN^k}{dt}(t) &= \frac{1}{2} \sum_{j_1=1}^k \sum_{j_2=1}^k f_{j_1 j_2}^k K_{j_1 j_2} N^{j_1} N^{j_2} - N^k \sum_{j=1}^{n_b} K_{kj} N^j \\ \frac{dQ_i^k}{dt}(t) &= \sum_{j_1=1}^k \sum_{j_2=1}^k f_{j_1 j_2}^k K_{j_1 j_2} Q_i^{j_1} N^{j_2} - Q_i^k \sum_{j=1}^{n_b} K_{kj} N^j \end{aligned} \quad (21)$$

$K_{j_1 j_2}$ is an approximation of the coagulation kernel between bins j_1 and j_2 .

The key point is to compute the partition coefficients $f_{j_1 j_2}^k$ that represent the fraction of particle combinations between bins j_1 and j_2 falling into bin k . As these coefficients only depend on the chosen discretization, they can be computed in a preprocessed step. The computation depends on the assumed shape of continuous densities inside each bin (for the closure scheme, see [Debry and Sportisse, 2006a](#)). In SIREAM, we use a closure scheme similar to [Fernández-Díaz et al. \(2000\)](#).

3.2.2 Condensation/evaporation-nucleation

Lagrangian formulation Let $\bar{x}^j(t)$ be the logarithmic mass of one particle at time t whose initial value corresponds to point x^j of the fixed discretization. The time evolution of $\bar{x}^j(t)$ is given by the equation of the characteristic curve:

$$5 \quad \frac{d\bar{x}^j}{dt}(t) = H_0(\bar{x}^j, t), \quad \bar{x}^j(0) = x^j \quad (22)$$

One crucial issue is to ensure that the characteristic curves do not cross themselves. If this happens the Lagrangian formulation is no longer valid. In real cases we have no proof that this does not happen, even though we have not seen such a situation up to now.

10 Provided that the characteristic curves do not cross, we can define integrated quantities N^j and Q_i^j for each Lagrangian bin $[\bar{x}^j, \bar{x}^{j+1}]$: $N^j(t) = \int_{\bar{x}^j}^{\bar{x}^{j+1}} n(x, t) dx$ and $Q_i^j = \int_{\bar{x}^j}^{\bar{x}^{j+1}} q_i(x, t) dx$.

Mass conservation can be easily written in the form: $c_i^g(t) + \sum_{j=1}^{n_b} Q_i^j(t) = K_i$.

The time derivation of integrated quantities leads to the equations:

$$15 \quad \frac{dN^j}{dt} = 0, \quad \frac{dQ_i^j}{dt} = N^j \tilde{l}_i^j \quad (23)$$

\tilde{l}_i^j is an approximation of the mass transfer rate for species X_i in bin j :

$$\tilde{l}_i^j = \underbrace{2\pi D_i d_p^j f(K_{n_i}^j, \alpha_i)}_{a_i^j} \left(K_i - \sum_{k=1}^{n_b} Q_i^k - \eta^j (c_i^{eq})^j \right) \quad (24)$$

with $\eta^j = e^{\frac{4\sigma v_p}{RT d_p^j}}$. $(c_i^{eq})^j$ is computed at \tilde{m}_i^j .

For the nucleation process, the first bound x^1 is assumed to correspond to the nucleation threshold, so that the Lagrangian bound \bar{x}^1 does not satisfy Eq. (22) but:

$$\frac{d\bar{x}^1}{dt} = j(t), \quad \bar{x}^1(0) = x^1 \quad (25)$$

where $j(t)$ is the growth law of the first bound due to nucleation and given by the nucleation parameterization. The equations for the first Lagrangian bin therefore are written as:

$$\frac{dN^1}{dt} = J_0(t), \quad \frac{dQ_i^1}{dt} = N^1 \tilde{f}_i^1 + m_i(x^1, t) J_0(t) \quad (26)$$

where $[m_1(x^1, t), \dots, m_{n_e}(x^1, t)]$ is the chemical composition of the nucleated particles, also given by the nucleation process.

The Lagrangian formulation consists in solving Eqs. (22), (23) and (26). In the next section we detail the various numerical strategies to perform the time integration, which is by far the most challenging point in particle simulation.

Interpolation of Lagrangian boundaries One has to solve the equations for the characteristic curves in order to know the boundaries of each bin. Notice that the c/e equations for boundaries are similar to those for integrated quantities. Indeed, for $j=1, \dots, n_b$ and $\tilde{x}^j = \ln(\tilde{m}^j)$, one gets from Eq. (23):

$$\frac{d\tilde{x}^j}{dt} = \tilde{H}_0^j, \quad \tilde{H}_0^j = \frac{\tilde{f}_0^j}{\tilde{m}^j}, \quad (27)$$

In practice, in order to reduce the computational burden, one tries to avoid solving boundary equations. An alternative is to interpolate the bin boundaries from integrated quantities.

One first method (Koo and Pandis, 2003) consists of utilizing the geometric mean of two adjacent bin:

$$\text{for } j = 2, \dots, n_b, \quad \tilde{m}^j(t) = \sqrt{\tilde{m}^{j-1}(t)\tilde{m}^j(t)} \quad (28)$$

This algorithm would have a physical meaning if Eqs. (22) and (27) were conserving formula (28), which is not the case. We have therefore developed another algorithm.

Equations (22) and (27) are similar and therefore \tilde{x}^j and \tilde{x}^{j-1} evolve in the same proportion given by $\lambda^j(t)$ ($j \geq 2$):

$$\lambda^j(t) = \frac{\tilde{x}^j(t) - \tilde{x}^{j-1}(t)}{\tilde{x}^j(t) - \tilde{x}^{j-1}(t)} \quad (29)$$

$\lambda^j(0)$ is known because $\tilde{x}^j(0) = x^j$. The time integration over $[0, t]$ of Eqs. (22) and (27) gives for $j \geq 1$:

$$\begin{aligned} \tilde{x}^j(t) &= x^j + \Delta \tilde{x}^j, \quad \Delta \tilde{x}^j = \int_0^t H_0^j(t') dt' \\ \tilde{x}^j(t) &= \tilde{x}^j(0) + \Delta \tilde{x}^j, \quad \Delta \tilde{x}^j = \int_0^t \tilde{H}_0^j(t') dt' \end{aligned} \quad (30)$$

The variation of each boundary \tilde{x}^j is then computed from that of its two adjacent bins \tilde{x}^{j-1} and \tilde{x}^j :

$$\Delta \tilde{x}^j \simeq (1 - \lambda^j(0))\Delta \tilde{x}^{j-1} + \lambda^j(0)\Delta \tilde{x}^j \quad (31)$$

where one assumes that λ^j remains constant.

Redistribution on a fixed size grid Using a Lagrangian approach for condensation/evaporation requires the redistribution or projection of number and mass concentrations onto the fixed size grid required by a 3-D model or for coagulation.

Let N and $(Q_i)_{i=1}^{n_e}$ be the integrated quantities of one Lagrangian bin after condensation/evaporation. We assume that this Lagrangian bin is covered by two adjacent fixed bins labelled j and $j+1$.

The redistribution algorithm must be conservative for the mass distribution of species X_i :

$$Q_j = Q_j^j + Q_j^{j+1} \quad (32)$$

Two algorithms have been developed: the first algorithm ensures that the number is conserved ($N=N^j+N^{j+1}$) while the second one ensures that the average mass is conserved.

1. If \bar{x}_{lo} and \bar{x}_{hi} are the boundaries of the Lagrangian bin after condensation/evaporation, the redistribution is performed as follows for the number distribution and the mass distribution of species X_i :

$$\begin{aligned} N^j &= \frac{\bar{x}_{hi}^j - \bar{x}_{lo}}{\bar{x}_{hi} - \bar{x}_{lo}} N, \quad Q_i^j = \frac{\bar{x}_{hi}^j - \bar{x}_{lo}}{\bar{x}_{hi} - \bar{x}_{lo}} Q \\ N^{j+1} &= \frac{\bar{x}_{hi} - \bar{x}_{lo}^{j+1}}{\bar{x}_{hi} - \bar{x}_{lo}} N, \quad Q_i^{j+1} = \frac{\bar{x}_{hi} - \bar{x}_{lo}^{j+1}}{\bar{x}_{hi} - \bar{x}_{lo}} Q \end{aligned} \quad (33)$$

Nevertheless the average mass of particles in each section (Q/N) may not be conserved by this algorithm.

2. Another approach consists in conserving the average mass. Let $\tilde{m}=Q/N$, $\tilde{m}^j=Q^j/N^j$ and $\tilde{m}^{j+1}=Q^{j+1}/N^{j+1}$ be the averaged mass of the Lagrangian bin and of bins j and $j+1$, respectively.

The algorithm for the number distribution and the mass distribution of species X_i

is given by:

$$\begin{aligned} N^j &= \frac{1 - \frac{\tilde{m}}{\tilde{m}^{j+1}}}{1 - \frac{\tilde{m}^j}{\tilde{m}^{j+1}}} N, \quad Q_i^j = \frac{\frac{\tilde{m}^{j+1}}{\tilde{m}} - 1}{\frac{\tilde{m}^{j+1}}{\tilde{m}^j} - 1} Q_i \\ N^{j+1} &= \frac{1 - \frac{\tilde{m}}{\tilde{m}^j}}{1 - \frac{\tilde{m}^{j+1}}{\tilde{m}^j}} N, \quad Q_i^{j+1} = \frac{1 - \frac{\tilde{m}^j}{\tilde{m}}}{1 - \frac{\tilde{m}^j}{\tilde{m}^{j+1}}} Q_i \end{aligned} \quad (34)$$

Both schemes are available in SIREAM.

5 3.3 Time integration

3.3.1 Coagulation

As coagulation is not a stiff process, we solve it by the second order explicit scheme ETR (Explicit Trapezoidal Rule) with the sequence:

$$\begin{aligned} \tilde{c}_{n+1} &= c_n + \Delta t f(c_n, t_n) \\ c_{n+1} &= c_n + \frac{\Delta t}{2} \left(f(c_n, t_n) + f(\tilde{c}_{n+1}, t_{n+1}) \right) \end{aligned} \quad (35)$$

with $c = (N^1, \dots, N^{n_b}, Q_1^1, \dots, Q_1^{n_b}, \dots, Q_{n_e}^1, \dots, Q_{n_e}^{n_b})$.

3.3.2 Condensation/evaporation

Here, $c = (Q_1^1, \dots, Q_{n_e}^1, \dots, Q_1^{n_b}, \dots, Q_{n_e}^{n_b})^T$. $n_c = n_e \times n_b$ is the dimension of c .

15 SIREAM offers three methods for solving condensation/evaporation: a fully dynamic method that treats dynamic mass transfer for each bin, a bulk equilibrium approach, and a hybrid approach that combines the two previous approaches.

Fully dynamic method Due to the wide range of timescales related to mass transfer, the system is stiff and implicit algorithms have to be used. The second-order Rosenbrock scheme (Verwer et al., 1999; Djouad et al., 2002), ROS2, is applied for the time integration:

$$\begin{aligned} 5 \quad c_{n+1} &= c_n + \frac{\Delta t_n}{2}(3k_1 + k_2) \\ [I - \gamma \Delta t_n J(f)]k_1 &= f(c_n, t_n) \\ [I - \gamma \Delta t_n J(f)]k_2 &= f(\tilde{c}_{n+1}, t_{n+1}) - 2k_1 \end{aligned} \quad (36)$$

where $\tilde{c}_{n+1} = c_n + \Delta t_n k_1$ and $\gamma = 1 + \frac{1}{\sqrt{2}}$.

This scheme requires the computation of the Jacobian matrix of f (a matrix $n_c \times n_c$) defined by $[J(f)]_{kl} = \frac{\partial f^k}{\partial c^l}$. f^k is the k -th component of function f and c^l is the l -th component of c .

Let us write $k = (i-1)n_b + j$ and $l = (i'-1)n_b + j'$ where i and i' label the semi-volatile species while j and j' label the bins. The (k/l) -th element of the Jacobian matrix may then be written as

$$15 \quad \frac{\partial f^k}{\partial c^l} = \frac{\partial I_i^j}{\partial Q_{i'}^{j'}} \quad (37)$$

The derivation of f^k may be split into one linear part, due to mass conservation, and one non-linear part related to the coefficient a_i^j , to the Kelvin effect η_i^j , and to the gas equilibrium concentration $(c_i^{eq})^j$. The linear part is analytically derived:

$$\left(\frac{\partial f^k}{\partial c^l} \right)_{\text{lin}} = -a_i^j N^{j'} \quad (38)$$

20 The non-linear part has to be differentiated by numerical methods, like the finite differ-

Title Page

Abstract

Introduction

Conclusions

References

Tables

Figures

◀

▶

◀

▶

Back

Close

Full Screen / Esc

Printer-friendly Version

Interactive Discussion

ence method:

$$\left(\frac{\partial f^k}{\partial c^l}\right)_{\text{non-lin}} = \frac{f^k(\dots, c^l(1 + \varepsilon_{\text{jac}}), \dots) - f^k(\dots, c^l, \dots)}{c^l \varepsilon_{\text{jac}}} \quad (39)$$

where ε_{jac} is generally close to 10^{-8} . During the numerical computation, the linear part is arbitrarily kept constant to avoid deriving it twice.

5 A default option, advocated for 3-D applications, is to approximate the Jacobian matrix by its diagonal. The motivation here is to reduce the CPU time.

Hybrid resolution Solving the c/e system, even with an implicit scheme, can be computationally inefficient. In order to lower the stiffness, hybrid methods for condensation/evaporation have been developed (Capaldo et al., 2000). The method consists in partitioning the state vector c into its fast components (c^f) and its slow components (c^s) respectively:

$$\frac{dc^s}{dt} = f^s(c^s, c^f, t), \quad f^f(c^s, c^f, t) = 0 \quad (40)$$

15 The algebraic equation states that the fast part is a function of the slow part, $c^f(t) = g(c^s(t), t)$. The time evolution of the slow part is now governed by:

$$\frac{dc^s}{dt} = f^s(c^s, g(c^s(t), t), t) \quad (41)$$

As c^s gathers particle species and sizes which have a slow c/e characteristic time, stiffness is substantially reduced.

20 The issue is now to determine whether particle sizes and species are “slow” or “fast”. The spectral study of the c/e system (Debry and Sportisse, 2006c) indicates how to compute a cutting diameter d_c between “slow” and “fast” species/sizes, such that the partitioning consists of cutting the particle distribution as follows: the smallest bins

are at equilibrium while the coarsest ones are governed by kinetic mass transfer. The cutting diameter can be computed by QSSA criteria, defined by:

$$\text{QSSA}_i^j = \frac{c_i^g - \eta_i^j (c_i^{\text{eq}})^j}{c_i^g + \eta_i^j (c_i^{\text{eq}})^j} \quad (42)$$

for a given chemical species X_i and one particle size j . The closer this ratio to zero, the closer the species and the size are to equilibrium.

In practice all bins j for which $(\text{QSSA}_i^j)_{j=1}^{n_\theta}$ is greater than one, the user parameter $\varepsilon_{\text{QSSA}}$ (close to unity) will be considered fast and solved by an equilibrium equation. In the following we write j_c as the bin corresponding to the cutting diameter. Bin j_c is the largest fast bin and bin j_c+1 is the smallest slow bin.

In SIREAM (to be used in 3D modeling), the default option is a fixed cutting diameter (1.25 or 2.5 μm).

The thermodynamic equilibrium between the gas phase and the fast particle bins is now written for species X_i as:

$$K_i^f - \sum_{j=1}^{j_c} Q_i^j - \eta_i^{j_c} c_i^{\text{eq}} (Q_1^k, \dots, Q_{n_\theta}^k) = 0 \quad (43)$$

with $K_i^f = K_i - \sum_{j=j_c+1}^{n_b} Q_i^j$ the total mass of species X_i for fast bins.

There are two approaches for solving this equilibrium: the bulk equilibrium approach and the size-resolved particle approach. For the size-resolved approach, we refer to [Jacobson et al. \(1996\)](#) (with the use of the fixed point algorithm) and to [Debry and Sportisse \(2006c\)](#) (with a minimization procedure).

In SIREAM, the bulk equilibrium has been implemented ([Pandis et al., 1993](#)). It

Title Page

Abstract

Introduction

Conclusions

References

Tables

Figures

◀

▶

◀

▶

Back

Close

Full Screen / Esc

Printer-friendly Version

Interactive Discussion

consists in merging all fast bins $j \leq j_c$ into one bin, referred as the “bulk” aerosol phase:

$$1 \leq i \leq n_e, \quad B_i = \sum_{j=1}^{j_c} Q_i^j \quad (44)$$

The thermodynamic model ISORROPIA is then applied to the “bulk” aerosol phase $(B_i)_{i=1}^{n_e}$ and one gets equilibrium “bulk” concentrations $(B_i^{eq})_{i=1}^{n_e}$ with the *forward* mode of the thermodynamics solver (global equilibrium).

The variation from initial to final “bulk” concentrations is then redistributed among fast bins $1 \leq k \leq j_c$ for species X_i (Pandis et al., 1993):

$$(Q_i^k)^{eq} = Q_i^k + b_i^k (B_i^{eq} - B_i), \quad b_i^k = \frac{a_i^k N^k}{\sum_{j=1}^{j_c} a_i^j N^j} \quad (45)$$

This redistribution scheme is exact provided that the particle composition is uniform over fast bins and that the variation of the particle diameter can be neglected for fast bins (Debry and Sportisse, 2006c).

Bulk approach It is a special case of the hybrid approach with the cutting diameter $j_c=1$ (all bins are at equilibrium).

4 Conclusions

We have summarized the main features of the aerosol model SIREAM (Size REsolved Aerosol Model). SIREAM simulates the GDE for atmospheric particles and can be easily linked to a three-dimensional Chemistry-Transport-Model. Moreover, the physical parameterizations used by SIREAM can be easily modified. They are currently hosted by the library ATMODATA and shared by another aerosol model (MAM, Sartelet et al., 2005).

A new Size REsolved Aerosol Model

E. Debry et al.

Title Page

Abstract

Introduction

Conclusions

References

Tables

Figures

◀

▶

◀

▶

Back

Close

Full Screen / Esc

Printer-friendly Version

Interactive Discussion

The next development steps are related to the improvement of the modeling of Secondary Organic Aerosol. The current parameterization of SOA is limited because it does not take into account the hydrophilic behavior of organic species (Griffin et al., 2002b,a; Pun et al., 2002). Furthermore new gas precursors such as isoprene and sesquiterpene should be added.

The modularity of SIREAM will be also strengthened by adding new alternative parameterizations (such as other thermodynamics models or simplified aqueous-phase chemical mechanisms) and new numerical algorithms (especially for time integration of condensation/evaporation).

A further step is also the extension to “externally mixed aerosol”.

Acknowledgements. Part of this project has been funded by the French Research Program, Primequal-Predit, in the framework of the PAM Project (Multiphase Air Pollution). Some of the authors (K. Fahey, K. Sartelet and M. Tombette) have been partially funded by the Region Ile de France.

References

- Binkowski, F. and Roselle, S.: Models-3 Community Multiscale Air Quality (CMAQ) model aerosol component. 1. Model description, J. Geophys. Res., 108(D6), 4183, doi:10.1029/2001JD001409, 2003. [11847](#)
- Brown, P., Byrne, G., and Hindmarsh, A.: VODE: A Variable Coefficient ODE Solver, SIAM J. on Sci. and Stat. Comp., 10, 1038–1051, 1989. [11859](#)
- Byun, D. and Schere, K.: EPA’s Third Generation Air Quality Modeling System: Description of the Models-3 Community, J. Mech. Rev., 2004. [11847](#)
- Capaldo, K., Pilinis, C., and Pandis, S.: A computationally efficient hybrid approach for dynamic gas/aerosol transfer in air quality models, Atmos. Environ., 34, 3617–3627, 2000. [11868](#)
- Dahneke, B.: Theory of Dispersed Multiphase Flow, Academic press, New York, 1983. [11851](#)
- Debry, E.: Numerical simulation of an atmospheric aerosol distribution, Ph.D. thesis, ENPC, CEREa, in French, 2004. [11860](#)
- Debry, E. and Sportisse, B.: Solving aerosol coagulation with size-binning methods, Appl. Numer. Math., accepted, 2006a. [11861](#)

A new Size REsolved Aerosol Model

E. Debry et al.

Title Page

Abstract

Introduction

Conclusions

References

Tables

Figures

◀

▶

◀

▶

Back

Close

Full Screen / Esc

Printer-friendly Version

Interactive Discussion

- Debry, E. and Sportisse, B.: Numerical simulation of the General Dynamics Equation (GDE) for aerosols with two collocation methods, Appl. Numer. Math., accepted, 2006b. [11860](#)
- Debry, E. and Sportisse, B.: Reduction of the condensation/evaporation dynamics for atmospheric aerosols: theoretical and numerical investigation of hybrid methods, J. Aerosol Sci., 37, 950–966, 2006c. [11868](#), [11869](#), [11870](#)
- Djouad, R., Sportisse, B., and Audiffren, N.: Numerical simulation of aqueous-phase atmospheric models: use of a non-autonomous Rosenbrock method, Atmos. Environ., 36, 873–879, 2002. [11867](#)
- Fahey, K.: Cloud and fog processing of aerosols: modeling the evolution of atmospheric species in the aqueous phase, Ph.D. thesis, Carnegie Mellon University, 2003. [11858](#)
- Fahey, K. and Pandis, S.: The role of variable droplet size-resolution in aqueous phase atmospheric chemistry modeling, in: Proceedings APMS 2001, edited by: Sportisse, B., Geosciences, Springer, 2001. [11858](#)
- Fernández-Díaz, J., González-Pola Muñiz, C., Rodríguez Braña, M., Arganza García, B., and García Nieto, P.: A modified semi-implicit method to obtain the evolution of an aerosol by coagulation, Atmos. Environ., 34, 4301–4314, 2000. [11861](#)
- Gaydos, T., Koo, B., Pandis, S., and Chock, D.: Development and application of an efficient moving sectional approach for the solution of the atmospheric aerosol condensation/evaporation equations, Atmos. Environ., 37, 3303–3316, 2003. [11849](#)
- Gelbard, F., Tambour, Y., and Seinfeld, J.: Sectional Representations for Simulating Aerosol Dynamics, J. Colloid Interface Sci., 76, 541–556, 1980. [11847](#)
- Gerber, H.: Relative-humidity parameterization of the Navy aerosol model (NAM), Tech. Rep. 8956, Natl. Res. Lab. Washington D.C., 1985. [11856](#)
- Griffin, R., Dabdub, D., Kleeman, M., Fraser, M., Cass, G., and Seinfeld, J.: Secondary organic aerosol 3. Urban/regional scale model of size- and composition-resolved aerosols, J. Geophys. Res., 107(D17), 4334, doi:10.1029/2001JD000544, 2002a. [11871](#)
- Griffin, R., Dabdub, D., and Seinfeld, J.: Secondary organic aerosol 1. Atmospheric chemical mechanism for production of molecular constituents, J. Geophys. Res., 1107(D17), 4332, doi:10.1029/2001JD000541, 2002b. [11871](#)
- Jacob, D.: Heterogeneous chemistry and tropospheric ozone, Atmos. Environ., 34, 2131–2159, 2000. [11859](#)
- Jacobson, M.: Analysis of aerosol interactions with numerical techniques for solving coagulation, nucleation, condensation, dissolution, and reversible chemistry among multiple size

A new Size REsolved Aerosol Model

E. Debry et al.

Title Page

Abstract

Introduction

Conclusions

References

Tables

Figures

◀

▶

◀

▶

Back

Close

Full Screen / Esc

Printer-friendly Version

Interactive Discussion

- distributions, J. Geophys. Res., 107(D19), 4366, doi:10.1029/2001JD002044, 2002. [11855](#)
- Jacobson, M., Tabazadeh, A., and Turco, R.: Simulating equilibrium within aerosols and nonequilibrium between gases and aerosols, J. Geophys. Res., 101, 9079–9091, 1996. [11869](#)
- 5 Koo, B. and Pandis, S.: Evaluation of the equilibrium, dynamic, and hybrid aerosol modeling approaches, Aerosol Sci. Technol., 37, 53–64, 2003. [11864](#)
- Korhonen, H., Lehtinen, K., Pirjola, L., Napari, I., Vehkamäki, H., Noppel, M., and Kulmala, M.: Simulation of atmospheric nucleation mode: a comparison of nucleation models and size distribution representations, J. Geophys. Res., 108(D15), 4471, doi:10.1029/2002JD003305, 2003. [11850](#)
- 10 Mallet, V. and Sportisse, B.: Data processing and parameterizations in atmospheric chemistry and physics: the AtmoData library, Tech. Rep., 2005-12, ENPC/CEREA, 2005. [11847](#), [11848](#)
- Mallet, V. and Sportisse, B.: Toward ensemble-based air-quality forecasts, J. Geophys. Res., accepted, 2006. [11848](#)
- 15 Meng, Z., Dabdub, D., and Seinfeld, J.: Size-resolved and chemically resolved model of atmospheric aerosol dynamics, J. Geophys. Res., 103, 3419–3435, 1998. [11849](#)
- Napari, I., Noppel, M., Vehkamäki, H., and Kulmala, M.: Parametrization of ternary nucleation rates for $\text{H}_2\text{SO}_4 - \text{NH}_3 - \text{H}_2\text{O}$ vapors, J. Geophys. Res., 107(D19), 4381, doi:10.1029/2002JD002132, 2002. [11850](#)
- 20 Nenes, A., Pandis, S., and Pilinis, C.: ISORROPIA: A new Thermodynamic Equilibrium Model for Multicomponent Inorganic Aerosols, Aquatic geochemistry, 4, 123–152, 1998. [11849](#)
- Pandis, S., Wexler, A., and Seinfeld, J.: Secondary organic aerosol formation and transport – II. Predicting the ambient secondary organic aerosol size distribution, Atmos. Environ., 27A, 2403–2416, 1993. [11869](#), [11870](#)
- 25 Pilinis, C. and Seinfeld, J.: Development and evaluation of an Eulerian photochemical gas-aerosol model, Atmos. Environ., 22, 1985–2001, 1988. [11855](#)
- Pilinis, C., Capaldo, K., Nenes, A., and Pandis, S.: MADM – a new Multi-component Aerosol Dynamic Model, Aerosol Sci. Technol., 32, 482–502, 2000. [11852](#)
- Pun, B., Griffin, R., Seigneur, C., and Seinfeld, J.: Secondary Organic Aerosol 2. Thermodynamic model for gas/particle partitioning of molecular constituents, J. Geophys. Res., 30 107(D17), 4333, doi:10.1029/2001JD000542, 2002. [11871](#)
- Sandu, A. and Borden, C.: A framework for the numerical treatment of aerosol dynamics, Appl. Numer. Math., 45, 475–497, 2003. [11860](#)

A new Size REsolved Aerosol Model

E. Debry et al.

Title Page

Abstract

Introduction

Conclusions

References

Tables

Figures

◀

▶

◀

▶

Back

Close

Full Screen / Esc

Printer-friendly Version

Interactive Discussion

- Sartelet, K. N., Hayami, H., Albriet, B., and Sportisse, B.: Development and preliminary validation of a Modal Aerosol Model for tropospheric chemistry: MAM, *Aerosol Sci. Technol.*, 40, 118–127, 2005. [11846](#), [11847](#), [11870](#)
- Schell, B.: Die Behandlung sekundärer organischer Aerosole in einem komplexen Chemie-Transport-Modell, Ph.D. thesis, Univ. Köln, 2000. [11853](#)
- Schell, B., Ackermann, I., Hass, H., Binkowski, F., and Ebel, A.: Modeling the formation of secondary organic aerosol within a comprehensive air quality model system, *J. Geophys. Res.*, 106(D22), 28 275–28 294, doi:10.1029/2001JD000384, 2001. [11853](#)
- Seigneur, C.: Current status of air quality modeling for particulate matter, *J. Air Waste Manage. Assoc.*, 51, 1508–1521, 2001. [11847](#)
- Seinfeld, J. and Pandis, S.: *Atmospheric Chemistry and Physics*, Wiley-interscience, 1998. [11846](#), [11850](#)
- Sportisse, B., Debry, E., Fahey, K., Roustan, Y., Sartelet, K., and Tombette, M.: PAM project (Multiphase Air Pollution): description of the aerosol models SIREAM and MAM, Tech. Rep. 2006-08, CEREa, available at: <http://www.enpc.fr/cerea/polyphemus>, 2006. [11847](#), [11856](#)
- Stockwell, W., Kirchner, F., Kuhn, M., and Seefeld, S.: A new mechanism for Regional Atmospheric Chemistry Modeling, *J. Geophys. Res.*, 95, 16 343–16 367, 1997. [11853](#)
- Strader, R., Gurciullo, C., Pandis, S., Kumar, N., and Lurmann, F.: Development of gas-phase chemistry, secondary organic aerosol and aqueous-phase chemistry modules for PM modeling, Tech. rep., STI, 1998. [11858](#)
- Vehkamäki, H., Kulmala, M., Napari, I., Lehtinen, K. E. J., Timmreck, C., Noppel, M., and Laaksonen, A.: An improved parameterization for sulfuric acid-water nucleation rates for tropospheric and stratospheric conditions, *J. Geophys. Res.*, 107(D22), 4622, doi:10.1029/2002JD002184, 2002. [11850](#)
- Verwer, J., Spee, E., Blom, J., and Hundsdorfer, W.: A second order Rosenbrock method applied to photochemical dispersion problem, *SIAM J. Sci. Comp.*, 20, 1456–1480, 1999. [11867](#)
- Wexler, A., Lurmann, W., and Seinfeld, J.: Modelling urban and regional aerosols – model development, *Atmos. Environ.*, 28, 531–546, 1994. [11849](#), [11855](#)
- Whitby, E. and McMurry, P.: Modal Aerosol Dynamics Modeling, *Aerosol Sci. Technol.*, 27, 673–688, 1997. [11847](#)
- Zhang, Y., Seinfeld, J., Jacobson, M., Clegg, S., and Binkowski, F.: A comparative review of inorganic aerosol thermodynamic equilibrium modules: similarities, differences and their

A new Size REsolved Aerosol Model

E. Debry et al.

Title Page

Abstract

Introduction

Conclusions

References

Tables

Figures

◀

▶

◀

▶

Back

Close

Full Screen / Esc

Printer-friendly Version

Interactive Discussion

likely causes, Atmos. Environ., 34(1), 117–137, 2000. [11852](#)
Zhang, Y., Pun, B., Vijayaraghavan, K., Wu, S., Seigneur, C., Pandis, S., Jacobson, M.,
Nenes, A., and Seinfeld, J.: Development and application of the Model of Aerosol Dy-
namics, Reaction, Ionization and Dissolution (MADRID), J. Geophys. Res., 109, D01202,
doi:10.1029/2003JD003501, 2004. [11847](#), [11850](#)

A new Size REsolved
Aerosol Model

E. Debry et al.

Title Page

Abstract

Introduction

Conclusions

References

Tables

Figures

◀

▶

◀

▶

Back

Close

Full Screen / Esc

Printer-friendly Version

Interactive Discussion